



## A novel information storage and visual expression device based on mechanoluminescence†

Cite this: *J. Mater. Chem. C*, 2019, 7, 4020

Received 1st February 2019,  
Accepted 27th February 2019

DOI: 10.1039/c9tc00641a

rsc.li/materials-c

Yong Zuo,<sup>‡,a</sup> Xiaojie Xu,<sup>‡,a</sup> Xin Tao,<sup>b</sup> Xiang Shi,<sup>a</sup> Xufeng Zhou,<sup>a</sup> Zhen Gao,<sup>a</sup>  
Xuemei Sun<sup>†</sup> \*<sup>a</sup> and Huisheng Peng<sup>†</sup> \*<sup>a</sup>

Information security has aroused wide concern in this new era of information; thus, the development of security methods for storing and expressing confidential information is of great importance. Herein, we provided a novel information storage and visual expression device based on mechanoluminescent materials and poly(dimethylsiloxane) using a simple fabrication method. The device could record the region where the stress was applied and store the information and finally express it *via* light emission under mechanical stimuli. Furthermore, the luminescence properties of the resulting device could be tuned by adjusting the composition of the mechanoluminescent layer or the initially applied stress. More importantly, the as-fabricated device exhibited a fast and sensitive response to the stimuli along with excellent repeatability as well as long-term stability, making it reliable for promising applications in confidential information storage, anti-counterfeiting and secure communication.

Information security is of vital significance for nations, society, and corporations as well as in personal life in the age of information; thus, it has attracted widespread and increasing research interests.<sup>1–4</sup> Based on this, extensive efforts have been made to develop efficient security methods to protect and store confidential information, and these range from markers,<sup>5,6</sup> holograms,<sup>7,8</sup> plasmonic labels,<sup>9,10</sup> radio frequency identification (RFID),<sup>11,12</sup> and chromism<sup>13,14</sup> to luminescence.<sup>15–20</sup> Particularly, luminescence is generally used as a security feature for information storage and expression due to its visualization, low cost and easy operation.<sup>21,22</sup> To date, much progress in developing photoluminescence (PL) materials, such as inorganic semiconductors,<sup>23–25</sup> organic dyes,<sup>26,27</sup> quantum dots,<sup>28,29</sup> and metal–organic frameworks (MOF),<sup>30,31</sup> has been made for applications in the field of information storage and expression. However, the visualization of PL materials is usually possible by UV light,

which exhibits some disadvantages, including the side effects on the human skin,<sup>32</sup> photobleaching or photodegradation<sup>33</sup> and the interference of the background fluorescence.<sup>34,35</sup> More importantly, the currently developed methods are considerably well-known to counterfeiters. Therefore, a novel, safe and stable technique is highly desired for information storage and visual expression. Mechanoluminescence is regarded as a clean, safe and reliable energy conversion mechanism for realizing light emission by mechanical stimuli without other irritation; it has attracted immense interests because of its wide applications in displays,<sup>36,37</sup> sensing,<sup>38,39</sup> e-signature,<sup>40</sup> and electronic skin.<sup>41</sup> However, to the best of our knowledge, mechanoluminescence exploited for information storage and expression has not been reported yet.

Herein, we demonstrated a novel information storage and visual expression device (ISVED) based on mechanoluminescence. Inspired by the need for daily information writing for recording, this concept was realized *via* information storage by pre-applying force to a particular area of the mechanoluminescent film and the information expression by exposing the film to other mechanical stimuli so as to excite visible-light emission. The light-emitting region was just where the stress was previously applied. The mechanoluminescent film contained metal-doped zinc sulfide (ZnS) microparticles as the luminescent materials and poly(dimethylsiloxane) (PDMS) as the elastic polymer matrix. The luminescence intensity could be tuned by regulating the composition of the composite film internally or by adjusting the applied force externally. More importantly, the device exhibited a quick response, good repeatability under periodical mechanical stimuli and long-term stability. The stimuli could be diverse including stretching, wind blowing and ultrasonication. Due to the simple process and the unique and promising advantages, such devices open up a new way in the fields of data storage, anti-counterfeiting and secure communication.

Fig. 1 schematically illustrates the working principle of ISVED. The device was prepared by evenly distributing mechanoluminescent materials into the soft elastomer matrix. When the device was subjected to an external force such as bending,

<sup>a</sup> State Key Laboratory of Molecular Engineering of Polymers, Department of Macromolecular Science, and Laboratory of Advanced Materials, Fudan University, Shanghai 200438, China. E-mail: sunxm@fudan.edu.cn, penghs@fudan.edu.cn

<sup>b</sup> Department of Materials Science, Fudan University, Shanghai 200438, China

† Electronic supplementary information (ESI) available. See DOI: 10.1039/c9tc00641a

‡ These authors contributed equally to this work.

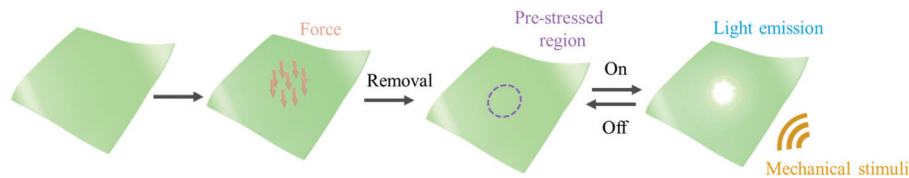


Fig. 1 Schematic for the working principle of ISVED.

folding, twisting and pressing, it underwent a certain degree of deformation. Meanwhile, small and unobvious structural variations might occur in the pre-stressed region. After the removal of the external load, the device could recover to the initial state macroscopically because of the excellent softness, elasticity and durability of the elastomer, while the invisible microstructure change of the pre-stressed region was retained. When the resulting device was further excited by mechanical stimuli such as stretching, wind blowing and ultrasonication, bright light was emitted from the pre-stressed location. In other words, the device is capable of remembering the position where it has experienced stress precisely and storing the changes invisibly, subsequently expressing them in visible light repeatedly by turning on/off the external stimuli.

A prototype was fabricated by embedding copper-doped zinc sulfide (ZnS:Cu) microparticles as mechanoluminescent materials into a soft PDMS elastomer matrix (Fig. 2a). The detailed preparation process is shown in the Experimental section. The ZnS:Cu microparticles with an average diameter of  $\sim 22 \mu\text{m}$  (Fig. S1, ESI<sup>†</sup>) were uniformly distributed within the PDMS matrix (Fig. S2, ESI<sup>†</sup>). In order to quantitatively investigate the force effect, the drop tower usually employed for mechanoluminescence measurements was selected (Fig. S3, ESI<sup>†</sup>).<sup>41</sup> Fig. 2b shows the composite film affected by the falling ball and the dotted circle indicates the pre-stressed region. After comparing the photographs shown in Fig. 2a and b, we inferred that there was no significant difference between the composite film before and after applying force. After immersing the device into an ultrasonic cleaner, a circle-shaped light-emitting spot appeared in the composite film (Fig. 2c). The light-emitting point was exactly where the stress had been applied. The device could also show the light-emitting point under other mechanical stimuli including stretching and wind blowing (Fig. S4, ESI<sup>†</sup>). If not specified, the devices were driven by ultrasonication due to its non-destruction in order to maintain the initial state of the devices.<sup>42</sup> The light disappeared immediately after turning off ultrasonication. However, the composite film without applying a force in advance showed no light emission when ultrasonication was turned on (Fig. S5, ESI<sup>†</sup>).

To shed light on the working mechanism of the device, its surface morphology was investigated. Fig. 2d shows the ultra-smooth surface of the nonluminous region in the device, whereas the surface of the light-emitting zone is rougher due to the exposure of microparticles, as shown in Fig. 2e. The performance of the smooth and rough area was investigated by a finite element modeling (FEM) simulation, which indicated stress distribution under strain (Fig. 2f). It revealed that the

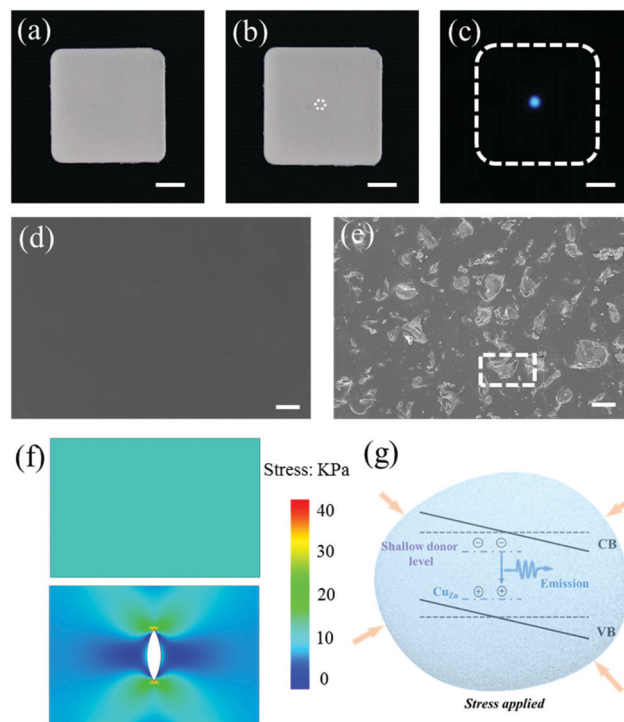


Fig. 2 Photographs and the working mechanism of the as-prepared device. Photographs of the obtained device before (a) and after (b) applying force. Dashes show the location with a pre-applied force. (c) Photograph of the obtained device excited by ultrasonication in the dark. Dashes represent the outline of the device. (d and e) SEM images of the non-luminous and luminous zones in the device. (f) Simulated stress distributions of the smooth area (top) and rough area with an exposed particle (bottom). (g) Schematic of the mechanism of the piezophotonic effect initiating the emission process. The scale bars in (a–c) and (d–e) are 0.5 cm and 20  $\mu\text{m}$ , respectively.

stress was redistributed and mainly concentrated on the poles of the gap generated by the pre-applied stress where ZnS:Cu microparticles were exposed. The widely accepted mechanism proposed for the mechanoluminescence process is the piezophotonic effect, a two-way coupling effect between piezoelectricity and photoexcitation properties, which induces the conversion process from mechanical stress to light emission.<sup>40,43</sup> When mechanical stress was applied to the device, the elastic matrix could transmit stress to the embedded ZnS:Cu grains and then, the conduction band (CB) and valence band (VB) of ZnS:Cu were tilted due to the piezoelectric potential. However, the electrons in the shallow donor levels below the conduction band were only excited if enough potential was originated from the mechanical stress transmitted from the elastic matrix.<sup>23</sup> As a result, if the

stress could be concentrated on certain positions of the elastic PDMS matrix, the stress that was actually transmitted to the ZnS:Cu microparticles therein *via* the elastomer was correspondingly larger so as to excite the electrons under the same external mechanical stimuli such as ultrasonication (Fig. S6, ESI<sup>†</sup>). After that, the excited electrons recombined with the holes trapped by the states of Cu impurities and then, an intense light was emitted (Fig. 2g).<sup>44</sup> Where there was stress concentration, there was light. Therefore, the applied stress was recorded and expressed visually.

In order to characterize the visual properties of these ISVEDs, two types of influences were taken into account. From the aspect of internal factors, three key parameters were discussed, namely, the content of ZnS:Cu particles, the elastic modulus of PDMS and the thickness of the composite film. As shown in Fig. 3a, the luminescence intensity of the device driven by ultrasonication increases rapidly as the content of ZnS:Cu particles increases from 20% to 70% due to the growing luminescent grains. The elastic modulus of PDMS could be tuned by changing the cross-linker ratio with prepolymers. For instance, the modulus of the device rapidly rose from 0.9 to 3.5 MPa along with the weight ratio of the cross-linker being increased from 3.6% to 10.0% (Fig. S7, ESI<sup>†</sup>). Then, the luminescence intensity was enhanced accordingly with the increasing weight ratio of the cross-linker (Fig. 3b), *i.e.*, the luminescence intensity of the device could be tuned by changing the elastic modulus of the polymer matrix.<sup>41</sup> Besides, the luminescence intensity was enhanced greatly when the thickness of the device was increased from 0.1 to 1 mm and then reached to sluggish after 1 mm or thicker (Fig. 3c). This was because more ZnS:Cu phosphor particles were activated. However, excessively thick devices with soft substrates could buffer the stress from the falling ball better, whereas the stress concentration in the device under stimuli was limited. Moreover, an

increase in thickness would block the light emission from bottom accompanied with increased opacity.

From the aspect of external factors, the initial external force that could be changed by adjusting the height of the falling object is a critical influential factor. When the pre-applied force reached 10 N, the light from the device under ultrasonication was visible to the naked eye and was detected by a photometer. The luminescence intensity of the devices with the same component and thickness increased linearly with the increase in force from 10 to 55 N (Fig. 3d). This could be ascribed to greater stress concentration caused by more gaps under a larger pre-applied force (Fig. S8, ESI<sup>†</sup>).

Fig. 3e presents the responsivity and repeatability of ISVED. In this measurement, the ultrasonic cleaner with a frequency of 42 kHz was initially switched on and held for 30 s and subsequently switched off periodically. The luminescence intensity increased to its saturation value immediately once ultrasonication was turned on and then declined towards zero rapidly when ultrasonication was turned off, indicating its fast response to external stimulus. Furthermore, the nearly unchanged luminescence intensity after 10 cycles (shown in Fig. 3e) also proved the regulation of visual information in reversible and dynamical manners with the stimuli on and off.

The stability of ISVED was also carefully studied by testing the luminescence intensity of the device every two days (Fig. 3f). It was clear that the intensity of ISVED displayed only a slight drop for half a month and the luminescent shape visible to the naked eye remained the same (Fig. S9, ESI<sup>†</sup>). Moreover, compared to the observation for the pre-stressed composite film, no distinct change in the surface morphology of ISVED was observed after stability tests (Fig. S10, ESI<sup>†</sup>). These results indicated the high stability for the expression of ISVED after a long period of storage, ensuring reliability for practical applications.

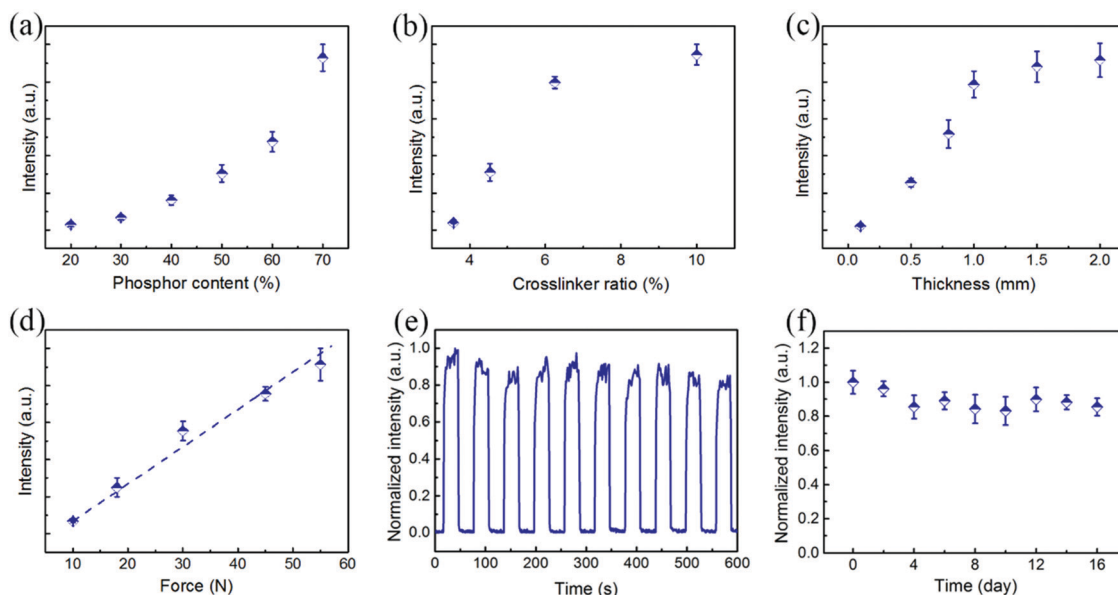
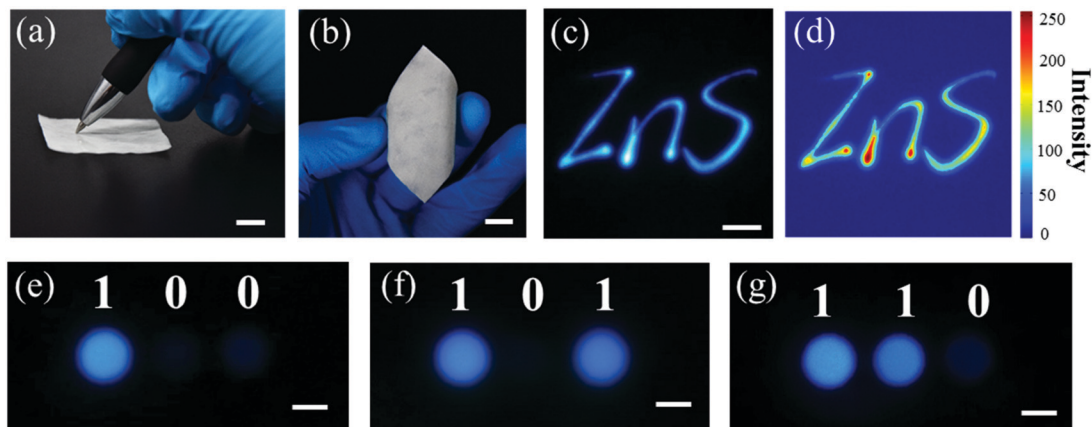


Fig. 3 Visual properties of ISVED. Dependence of the luminescence intensity of ISVED on the phosphor content (a), cross-linker ratio of PDMS matrix (b), thickness (c) and pre-applied external force (d). (e) The responsivity and repeatability of ISVED. (f) Stabilities of ISVED.



**Fig. 4** Demonstrations of the application of the device. (a) Photograph of writing information on the device. (b) Photograph of the device written with “ZnS” word under daylight. (c) Photograph of the device excited by ultrasonication in the dark. (d) The corresponding distribution of luminescence intensity in (c). (e–g) Photographs of the binary coding chips based on ISVEDs with various patterns excited by ultrasonication in the dark. The scale bars in (a and b), (c) and (e–g) are 1 cm, 5 mm and 1 mm, respectively.

Based on the above investigations, we infer that ISVED is desirable for information encryption and decryption. As paper is still the foremost carrier of information storage in spite of the rapid development of electronic communications,<sup>45</sup> herein, we brushed the PDMS precursor and ZnS:Cu microparticle composite onto a commercial clean paper for laboratory use simply (Fig. S11, ESI†). The load could be regulated by changing the total coating weight of the mechanoluminescent mixture. Here, about 1.2 g composite containing PDMS precursor and ZnS:Cu microparticles was brushed onto a 4 × 4 cm paper. The obtained paper-based ISVED demonstrated light weight, excellent flexibility and portability (Fig. S12, ESI†). Fig. 4a shows that the word “ZnS” can be written on the as-fabricated device by a pen. Obviously, the written pattern was invisible under daylight and UV light with the naked eye (Fig. 4b and Fig. S13, ESI†). When the device was immersed into the solution of a working ultrasonic cleaner, the handwritten word “ZnS” with a bright blue light was revealed directly (Fig. 4c). The intensity distribution of luminescence was analyzed by extracting the gray scale values of the obtained image (Fig. 4d), which clearly mapped the different intensity distributions of every letter due to varied writing strengths. Obviously, the letter “n” was distinctly written with a stronger force at the beginning and end. It is well-known that the writing style of one writer is not identical to that of anybody else (Fig. S14, ESI†); thus, ISVED has the capability of recording and storing detailed signing information from handwritten signatures, which is promising for personalized signature collection and anti-counterfeiting applications.

Moreover, binary coding chips for 2-logic state data storage can be realized by applying different stresses on the patterned points of ISVEDs. As a demonstration, three spots were patterned on ISVEDs to store confidential information, which were invisible to the naked eyes under visible and UV lights (Fig. S15, ESI†). By placing the chips in an ultrasonic field, distinct light emissions were produced (Fig. 4e–g). If bright and weak luminescent spots represented “1” and “0”, respectively, the binary coding information could be easily obtained by translating

numbers from optical signals. The stored information of “100”, “101” and “110” is shown clearly in Fig. 4e–g, revealing the tremendous potential for applications in data storage and secure communication.

## Conclusions

In summary, a new information storage and visual expression device was developed based on mechanoluminescence by applying a force to a ZnS:Cu-embedded PDMS composite film in advance. The device could precisely record the region where the stress was applied and store it. Afterwards, the information could be expressed in a visualized way of light emission when activated by external mechanical stimuli. More importantly, the device equipped with excellent responsivity, repeatability and stability under nondestructive ultrasound stimuli demonstrated great potential for hiding confidential information and communicating securely. This work provides an effective method for information storage and visual expression, which is beneficial to several individuals and organizations.

## Experimental section

### Fabrication of the devices

Commercially available alumina-coated ZnS:Cu phosphor particles (Shanghai Keyan Phosphor Technology Company Limited) were mixed with PDMS (Wacker ELASTOSIL RT601) in the weight ratio of 7 : 3. After degassing in a vacuum oven, the mixtures were poured into a customized mould and then cured in an oven box at 80 °C for about 20 min. The devices for experiment were obtained after the removal of the mould.

### Experimental setup

Using the drop tower described in the literature related to mechanoluminescence,<sup>41</sup> the film was impacted by a falling

ball. The steel ball was dropped from different heights, and the force was quantified by a pressure sensor under the film.

### Characterization

The morphologies of the films were investigated using a field-emission scanning electron microscope (Ultra 55, Zeiss), which was operated at 5 kV. The images were captured by a digital camera (D3400, NIKON). The luminescence properties of the composite films excited by an ultrasonic cleaner (CE-6200A, Jeken) were measured with a photometer (Admesy Asteria). The stress-strain characteristics of different films with various weight ratios of cross-linker were obtained by a Hengyi Table-Top universal testing instrument.

### Simulation of the local stress distributions

The model was built with a finite element software ABAQUS to simulate the stress distribution of composite film with or without one gap. In the model, the gap was fusiform, which was a common and basic shape in the real sample, and the elastic modulus and Poisson's ratio of the composite film were 3.5 MPa and 0.3, respectively. The type of mesh elements was linear hexahedral and the total number was 36 416. The load was applied to both sides of the film.

### Conflicts of interest

The authors declare no conflicts of interest.

### Acknowledgements

This work was supported by MOST (2016YFA0203302), NSFC (21634003, 51573027, 51673043, 21604012, 21805044, 21875042), STCSM (16JC1400702, 17QA1400400, 18QA1400700, 18QA1400800), SHMEC (2017-01-07-00-07-E00062) and Yanchang Petroleum Group.

### Notes and references

- B. L. Volodin, B. Kippelen, K. Meerholz, B. Javidi and N. Peyghambarian, *Nature*, 1996, **383**, 58–60.
- M. T. Dlamini, J. H. P. Eloff and M. M. Eloff, *Comput. Secur.*, 2009, **28**, 189–198.
- B. Yoon, J. Lee, I. S. Park, S. Jeon, J. Lee and J. M. Kim, *J. Mater. Chem. C*, 2013, **1**, 2388–2403.
- T. Sarkar, K. Selvakumar, L. Motiei and D. Margulies, *Nat. Commun.*, 2016, **7**, 11374.
- H. J. Bae, S. Bae, C. Park, S. Han, J. Kim, L. N. Kim, K. Kim, S. Song, W. Park and S. Kwon, *Adv. Mater.*, 2015, **27**, 2083–2089.
- K. J. Si, D. Sikdar, L. W. Yap, J. Kee, K. Foo and P. Guo, *Adv. Opt. Mater.*, 2015, **3**, 1710–1717.
- W. Ye, F. Zeuner, X. Li, B. Reineke, S. He, C. Qiu, J. Liu, Y. Wang, S. Zhang and T. Zentgraf, *Nat. Commun.*, 2016, **7**, 11930.
- G. Ruffato, R. Rossi, M. Massari, E. Mafakheri, P. Capaldo and F. Romanato, *Sci. Rep.*, 2017, **7**, 18011.
- Y. Zheng, C. Jiang, S. H. Ng, Y. Lu, F. Han, U. Bach and J. J. Gooding, *Adv. Mater.*, 2016, **28**, 2330–2336.
- X. Duan, S. Kamin and N. Liu, *Nat. Commun.*, 2017, **8**, 14606.
- C. M. Roberts, *Comput. Secur.*, 2006, **25**, 18–26.
- M. Benssalah, M. Djeddou and K. Drouiche, *Wirel. Pers. Commun.*, 2017, **96**, 6221–6238.
- P. Xue, Z. Yang and P. Chen, *J. Mater. Chem. C*, 2018, **6**, 4994–5000.
- M. Qiu, P. Sun, B. Zhang, J. Yu, Y. Fu, X. Yu, C. Zhao and W. Mai, *Adv. Opt. Mater.*, 2018, **6**, 1800338.
- C. Shi, Y. Zhu, G. Zhu, X. Shen and M. Ge, *J. Mater. Chem. C*, 2018, **6**, 9552–9560.
- P. Kumar, J. Dwivedi and B. K. Gupta, *J. Mater. Chem. C*, 2014, **2**, 10468–10475.
- P. Kumar, S. Singh and B. K. Gupta, *Nanoscale*, 2016, **8**, 14297–14340.
- C. Wang, Y. Jin, Y. Lv, G. Ju, D. Liu, L. Chen, Z. Li and Y. Hu, *J. Mater. Chem. C*, 2018, **6**, 6058–6067.
- Y. Ma, S. Liu, H. Yang, Y. Zeng, P. She, N. Zhu, C. L. Ho, Q. Zhao, W. Huang and W. Y. Wong, *Inorg. Chem.*, 2017, **56**, 2409–2416.
- Y. Ma, P. She, K. Y. Zhang, H. Yang, Y. Qin, Z. Xu, S. Liu, Q. Zhao and W. Huang, *Nat. Commun.*, 2018, **9**, 3.
- K. Liu, C. Shan, G. He, R. Wang, Z. Sun, Q. Liu, L. Dong and D. Shen, *J. Mater. Chem. C*, 2017, **5**, 7167–7173.
- V. K. Singh, R. K. Chitumalla, S. K. Ravi, Y. Zhang, Y. Xi, V. Sanjairaj, C. Zhang, J. Jang and S. C. Tan, *ACS Appl. Mater. Interfaces*, 2017, **9**, 33071–33079.
- X. Xu, S. Li, J. Chen, S. Cai, Z. Long and X. Fang, *Adv. Funct. Mater.*, 2018, **28**, 1802029.
- X. Shi, X. Zhou, Y. Zhang, X. Xu, Z. Zhang, P. Liu, Y. Zuo and H. Peng, *J. Mater. Chem. C*, 2018, **6**, 12774–12780.
- X. Xu, L. Hu, N. Gao, S. Liu, S. Wageh, A. A. Al-Ghamdi, A. Alshahrie and X. Fang, *Adv. Funct. Mater.*, 2015, **25**, 445–454.
- P. Wei, B. Li, A. De Leon and E. Pentzer, *J. Mater. Chem. C*, 2017, **5**, 5780–5786.
- Y. Su, S. Z. F. Phua, Y. Li, X. Zhou, D. Jana, G. Liu, W. Q. Lim, W. K. Ong, C. Yang and Y. Zhao, *Sci. Adv.*, 2018, **4**, eaas9732.
- Z. Song, T. Lin, L. Lin, S. Lin, F. Fu, X. Wang and L. Guo, *Angew. Chem., Int. Ed.*, 2016, **55**, 2773–2777.
- Z. Lu, Y. Liu, W. Hu, X. Lou and C. Li, *Chem. Commun.*, 2011, **47**, 9609–9611.
- C. Zhang, B. Wang, W. Li, S. Huang, L. Kong, Z. Li and L. Li, *Nat. Commun.*, 2017, **8**, 1138.
- Y. Wang, X. Tian, H. Zhang, Z. Yang and X. Yin, *ACS Appl. Mater. Interfaces*, 2018, **10**, 22445–22452.
- X. Xu, J. Chen, S. Cai, Z. Long, Y. Zhang, L. Su, S. He, C. Tang, P. Liu, H. Peng and X. S. Fang, *Adv. Mater.*, 2018, **30**, 1803165.
- L. Zhu, M. Zhu, J. K. Hurst and A. D. Q. Li, *J. Am. Chem. Soc.*, 2005, **127**, 8968–8970.
- Y. Lu, J. Zhao, R. Zhang, Y. Liu, D. Liu, E. M. Goldys, X. Yang, P. Xi, A. Sunna, J. Lu, Y. Shi, R. C. Leif, Y. Huo, J. Shen, J. A. Piper, J. P. Robinson and D. Jin, *Nat. Photonics*, 2014, **8**, 32–36.

- 35 Q. Ma, J. Wang, Z. Li, D. Wang, X. Hu, Y. Xu and Q. Yuan, *Inorg. Chem. Front.*, 2017, **4**, 1166–1172.
- 36 J. Zhang, L. Bao, H. Lou, J. Deng, A. Chen, Y. Hu, Z. Zhang, X. Sun and H. Peng, *J. Mater. Chem. C*, 2017, **5**, 8027–8032.
- 37 S. M. Jeong, S. Song, K. I. Joo, J. Kim, S. H. Hwang, J. Jeong and H. Kim, *Energy Environ. Sci.*, 2014, **7**, 3338–3346.
- 38 C. Xu, T. Watanabe, M. Akiyama and X. Zheng, *Appl. Phys. Lett.*, 1999, **74**, 2414–2416.
- 39 C. Xu, X. Zheng, M. Akiyama, K. Nonaka and T. Watanabe, *Appl. Phys. Lett.*, 2000, **76**, 179–181.
- 40 X. Wang, H. Zhang, R. Yu, L. Dong, D. Peng, A. Zhang, Y. Zhang, H. Liu, C. Pan and Z. L. Wang, *Adv. Mater.*, 2015, **27**, 2324–2331.
- 41 X. Qian, Z. Cai, M. Su, F. Li, W. Fang, Y. Li, X. Zhou, Q. Li, X. Feng, W. Li, X. Hu, X. Wang, C. Pan and Y. Song, *Adv. Mater.*, 2018, **30**, 1800291.
- 42 H. Hu, X. Zhu, C. Wang, L. Zhang, X. Li, S. Lee, Z. Huang, R. Chen, Z. Chen, C. Wang, Y. Gu, Y. Chen, Y. Lei, T. Zhang, N. Kim, Y. Guo, Y. Teng, W. Zhou, Y. Li, A. Nomoto, S. Sternini, Q. Zhou, M. Pharr, F. Lanza and S. Xu, *Sci. Adv.*, 2018, **4**, eaar3979.
- 43 Z. L. Wang, *Nano Today*, 2010, **5**, 540–552.
- 44 S. W. Shin, J. P. Oh, C. W. Hong, E. M. Kim, J. J. Woo, G. Heo and J. H. Kim, *ACS Appl. Mater. Interfaces*, 2016, **8**, 1098–1103.
- 45 W. Jeong, M. I. Khazi, D. Park, Y. Jung and J. Kim, *Adv. Funct. Mater.*, 2016, **26**, 5230–5238.